

Broken-Symmetry States of Dirac Fermions in Graphene with a Partially Filled High Landau Level

Hao Wang,¹ D. N. Sheng,¹ L. Sheng,² and F. D. M. Haldane³

¹*Department of Physics and Astronomy, California State University, Northridge, California 91330, USA*

²*National Laboratory of Solid State Microstructures and Department of Physics, Nanjing University, Nanjing 210093, People's Republic of China*

³*Department of Physics, Princeton University, Princeton, New Jersey 08544, USA*

(Received 8 August 2007; published 20 March 2008)

We report on numerical study of the Dirac fermions in partially filled $N = 3$ Landau level (LL) in graphene. At half-filling, the equal-time density-density correlation function displays sharp peaks at nonzero wave vectors $\pm \mathbf{q}^*$. Finite-size scaling shows that the peak value grows with electron number and diverges in the thermodynamic limit, which suggests an instability toward a charge density wave. A symmetry broken stripe phase is formed at large system size limit, which is robust against perturbation from disorder scattering. Such a quantum phase is experimentally observable through transport measurements. Associated with the special wave functions of the Dirac LL, both stripe and bubble phases become possible candidates for the ground state of the Dirac fermions in graphene with lower filling factors in the $N = 3$ LL.

DOI: [10.1103/PhysRevLett.100.116802](https://doi.org/10.1103/PhysRevLett.100.116802)

PACS numbers: 73.43.-f, 71.10.-w, 71.45.Lr, 73.22.Gk

Recently, successful fabrication of single-atomic-layer-thick films of graphite [1], called graphene, has triggered intensive research activities to understand the novel properties [2–6] of these new two-dimensional (2D) electron systems (2DES's). Different from the conventional 2D electrons with the quadratic dispersion relation, the low-energy electron excitations in graphene have a linear (relativistic) dispersion relation, which can be described by a massless Dirac equation [7–9]. The Dirac-fermion-like nature of the electrons has manifested itself evidently in the unconventional quantization pattern of integer quantum Hall effect (IQHE) [2–6, 10–13]. The possibilities to observe the fractional quantum Hall effect in graphene in the partially filled $N = 0$ and $N = 1$ LLs and a pseudospin ferromagnetic state in the $N = 1$ LL have been predicted in some recent theoretical works [12–15], which, however, have not been experimentally observed yet. Thus the role of impurity scattering seems crucially important, which may obscure the observation of these quantum phases for currently available sample mobility. At even higher LLs, there exist many studies on the conventional 2DES's, where a variety of quantum phases have been predicted [16–19] and discovered experimentally [20], varying from stripe phase to reentrant QHE. On the other hand, for the Dirac fermions with partially filled high LLs in graphene, investigations are only carried out based on the Hartree-Fock mean-field approximation [21], which suggested that stripe and bubble phases are possible. It remains an open issue whether such quantum phases can survive quantum fluctuations and disorder scattering. Study of the quantum phases of Dirac fermions in high LLs is highly valuable for elucidating the key role of the Coulomb interaction and the disorder effect in graphene.

In this Letter, we investigate the low-energy states of the Dirac fermions in graphene with partially filled $N = 3$ Dirac LL using the Lanczos method for finite-size systems with torus geometry and up to $N_e = 16$ electrons in the LL [22]. For a pure system at half-filling, we find a large number of nearly degenerate low-energy states, which are equally distanced from each other by a characteristic wave vector \mathbf{q}^* in momentum space. The equal-time density-density correlation function shows strong and sharp peaks at $\pm \mathbf{q}^*$, indicating the charge density wave (CDW) instability. Finite-size scaling shows that the peak value grows with electron number and becomes divergent in the thermodynamic limit. Thus a symmetry broken stripe phase will be formed at large system size limit, which is robust against moderate disorder scattering with a critical disorder strength comparable with that for the nonrelativistic 2DES's [23]. Because of the special single-particle wave functions of the Dirac LL, both stripe and bubble phases are possible candidates for the ground state with lower filling factors in the $N = 3$ LL based on exact calculations. We further discuss the transport anisotropy of the stripe phase, which can be used to experimentally detect this quantum phase.

We consider a 2DES in an $L_x \times L_y$ rectangular cell of graphene under a perpendicular magnetic field. The magnetic length ℓ is taken to be the unit of length. The total number of flux quanta $N_\phi = L_x L_y / 2\pi$ is chosen to be an integer. Periodic boundary conditions are imposed in both x and y directions [18]. The magnetic field is assumed to be strong enough so that the spin degeneracy of the LLs is lifted, and all the LLs are well separated from each other. One can thus project the system Hamiltonian into the topmost, partially filled, N th LL [18]. The projected

Hamiltonian, which contains the Coulomb interaction and disorder potential, has the form

$$H_c = \sum_{i < j} \sum_{\mathbf{q}} e^{-q^2/2} [F_N(q)]^2 V(q) e^{i\mathbf{q} \cdot (\mathbf{R}_i - \mathbf{R}_j)} / 2\pi N_\phi + \sum_i \sum_{\mathbf{q}} e^{-q^2/4} F_N(q) V_{\text{imp}}(q) e^{i\mathbf{q} \cdot \mathbf{R}_i}, \quad (1)$$

where \mathbf{R}_i is the guiding center coordinate (GCC) of the i th electron, and $V(q) = 2\pi e^2 / \epsilon q$ is the Fourier transform of the Coulomb interaction. The wave vector \mathbf{q} takes discrete values that are compatible with the geometry of the system. Noticing that the electron wave function in a relativistic Dirac LL of N is a mixture of two wave functions in two different nonrelativistic LLs of N and $N - 1$, we can write the form factor $F_N(q)$ in Eq. (1) as [12]

$$F_N(q) = \frac{1}{2} [L_N(q^2/2) + L_{N-1}(q^2/2)], \quad (2)$$

where $L_N(x)$ is the Laguerre polynomial. The disorder potential is generated according to the correlation relation in q space $\langle V_{\text{imp}}(q) V_{\text{imp}}(-q') \rangle = \frac{W^2}{L_x L_y} \delta_{q, -q'}$, which corresponds to $\langle V_{\text{imp}}(\mathbf{r}) V_{\text{imp}}(\mathbf{r}') \rangle = W^2 \delta(\mathbf{r} - \mathbf{r}')$ in real space with W as the strength of disorder in units of $e^2 / \epsilon \ell$.

We compute exactly the low-energy spectrum and wave functions using the Lanczos diagonalization method. We

find that pseudospin-polarized states have lower energies than unpolarized states. In Fig. 1(a), the low-energy spectrum for the $N = 3$ LL with filling factor $\nu = 1/2$ and $N_e = 12$ is shown as a function of the aspect ratio $\text{asp} = L_x / L_y$. Here, the filling factor is defined as $\nu = N_e / N_\phi$ with N_e the electron number in the LL. A generic feature of the spectrum is the existence of a number of nearly degenerate low-energy states well separated from higher-energy states by a gap, in a wide range of aspect ratio $0.7 < \text{asp} < 0.9$. We will call these states the ground-state manifold. In Fig. 1(b), we plot the low-energy spectrum as a function of wave vector q_y at the optimized aspect ratio $\text{asp} = 0.74$, where the energy broadening of the manifold is minimized. All the states in the manifold are equally separated from each other by a characteristic wave vector $\mathbf{q}^* = (0, q_y^*)$ with $q_y^* = 4\pi / L_y$. This feature is similar to that observed in the spectra of the nonrelativistic 2DES's with half-filled high LLs [18], which indicates an instability towards a unidirectional CDW or stripe phase.

We next turn to the LL projected equal-time density-density correlation function $S_0(\mathbf{q})$ of the ground state [18]. In Fig. 2(a), $S_0(\mathbf{q})$ for the half-filled $N = 3$ LL with $N_e = 12$ and aspect ratio $\text{asp} = 0.74$ is shown in a 3D plot. We see that there are two sharp and strong peaks at $\pm \mathbf{q}^* = (0, \pm 0.88)$ with the peak value 4.37, while $S_0(q)$ is about

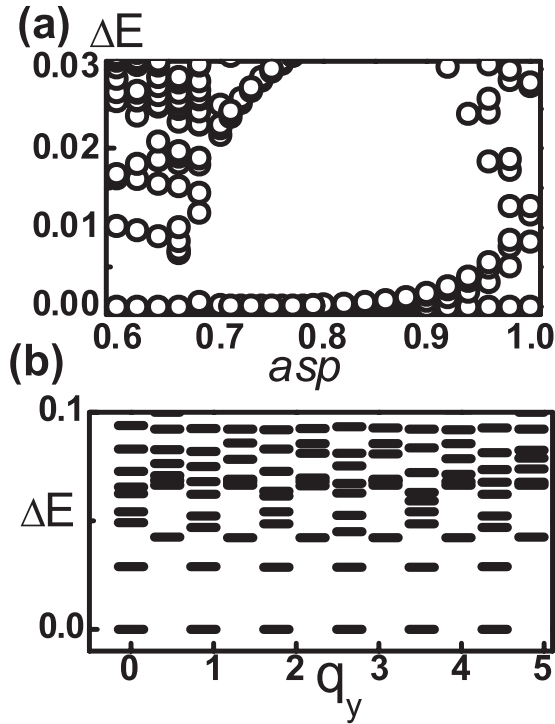


FIG. 1. Low-energy spectrum for the half-filled $N = 3$ LL with $N_e = 12$ in a clean system. (a) Energy levels versus aspect ratio asp , where the eigenenergies are measured in units of $e^2 / \epsilon \ell$ with respect to the ground state. (b) Energy levels versus the y component of wave vector at aspect ratio $\text{asp} = 0.74$. The six nearly degenerate lowest-energy states are equally separated by a wave vector $\mathbf{q}^* = (0, 4\pi / L_y) = (0, 0.88)$.

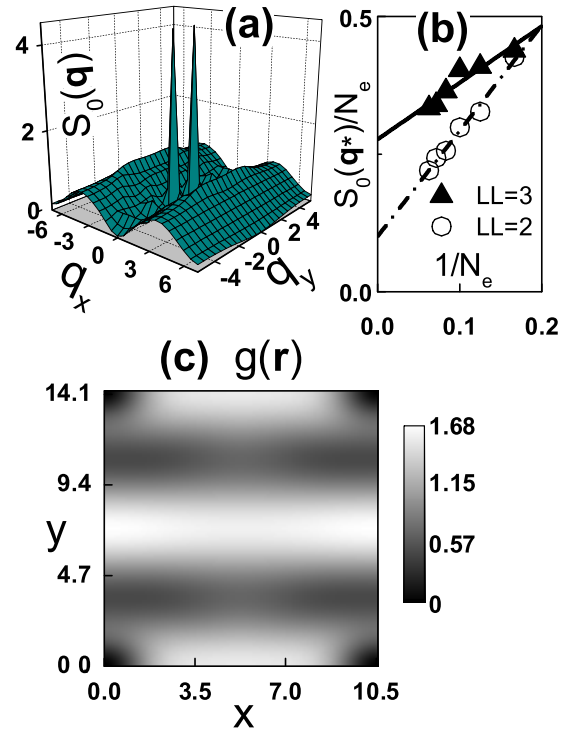


FIG. 2 (color online). Correlation functions of the ground state for the half-filled $N = 3$ LL in a clean system. (a) Static density-density correlation function $S_0(\mathbf{q})$ with $N_e = 12$ and $\text{asp} = 0.74$. (b) Peak value of $S_0(\mathbf{q})$ normalized by N_e as a function of $1/N_e$ for $N = 2$ and 3 LLs. (c) Ground-state pair correlation function $g(\mathbf{r})$ in guiding center coordinates with $N_e = 12$ and $\text{asp} = 0.74$.

0.5 away from the peaks. The presence of the peaks in $S_0(\mathbf{q})$ at \mathbf{q}^* suggests strong density correlation at the ordering wave vector, which is consistent with the characteristic feature of the low-energy spectrum. We have also examined $S_0(\mathbf{q})$ at a number of other aspect ratios in the range of $0.7 < \text{asp} < 0.9$, which all show sharp peaks but with slightly reduced peak values. The ratio $\frac{S_0(\mathbf{q}^*)}{N_e}$ for different electron numbers from $N_e = 6$ up to $N_e = 16$ is shown as a function of $1/N_e$ in Fig. 2(b), at the corresponding optimized aspect ratios. The ratio $\frac{S_0(\mathbf{q}^*)}{N_e}$ extrapolates linearly to a finite value 0.28 as $N_e \rightarrow \infty$, which is proportional to the relative density modulation in the symmetry broken state. Therefore, the instability towards a unidirectional CDW phase in large systems is established by finite-size scaling. We have also studied the $N = 2$ LL, where both the value of $S_0(\mathbf{q}^*)$ and the value of $\frac{S_0(\mathbf{q}^*)}{N_e}$ at $N_e \rightarrow \infty$ are smaller than those in the $N = 3$ LL case suggesting the $N = 3$ LL to be the better candidate for observing the CDW phases in graphene.

The CDW order of the above ground state in the real space is studied using the LL projected pair correlation function $g(r)$ [24]. In Fig. 2(c), we plot the ground-state pair correlation function in GCC for the half-filled $N = 3$ LL with $N_e = 12$ and $\text{asp} = 0.74$. It shows clearly that there are two stripes inside the unit cell along the x direction. The mean separation between the two stripes is related to the ordering wave vector q_y^* through $D_s = 2\pi/q_y^* = 7.1$, which happens to be a half of L_y for the present system. By examining systems with N_e ranging from 6 up to 16 at their optimized aspect ratios, we find that the ordering wave vector q_y^* changes slightly with N_e between $q_y^* = 0.88$ and 0.96 , and correspondingly D_s varies between 6.5 and 7.1 magnetic lengths, which are comparable to the ones for the nonrelativistic 2DES's [18].

The above calculated correlation functions establish a stripe phase at the thermodynamic limit, in agreement with the Hartree-Fock result [21]. We also note that in a clean finite-size system ($W = 0$), the ground-state wave function is invariant under the magnetic translation of guiding centers of the cyclotron orbits, while the symmetry broken stripe phase can become the true ground state when a relatively weak disorder is turned on [23]. In the presence of such random disorder, we can directly probe the CDW phase using the LL projected local electron density $\rho(\mathbf{r})$ [23]. For a very weak disorder strength, the typical behavior of $\rho(\mathbf{r})$ is shown in Fig. 3(a), where $W = 0.01$. Two nearly perfect stripes are formed along the x direction with essentially no density modulations along the stripes. At an intermediate disorder strength $W = 0.1$, there are still two complete stripes, though the shape of the stripes exhibits pronounced variations along the stripe direction. Thus we conclude that for weak to moderate disorder strength, the ground state is in the quantum Hall stripe phase. With further increasing disorder strength, as shown in Fig. 3(c) for $W = 0.2$, the stripe density profile becomes ruptured

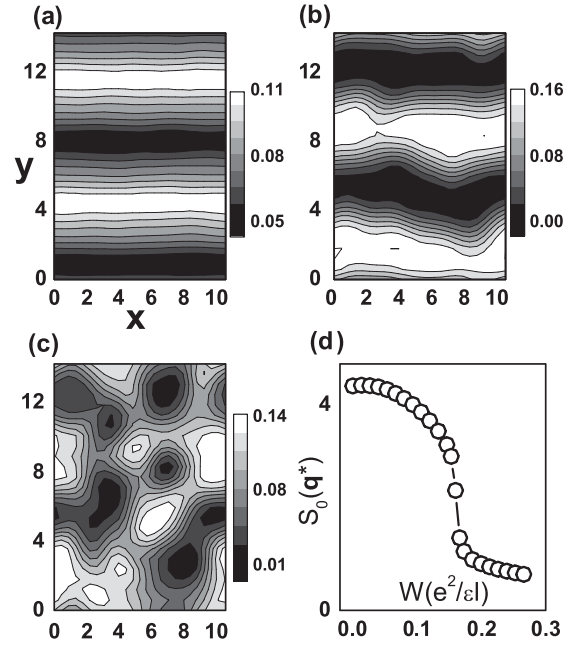


FIG. 3. Disorder effect on the ground state of the half-filled $N = 3$ LL with $N_e = 12$ and $\text{asp} = 0.74$. Projected electron density $\rho(\mathbf{r})$ at disorder strengths (a) $W = 0.01$, (b) $W = 0.10$, and (c) $W = 0.20$. (d) Peak value of $S_0(\mathbf{q})$ versus disorder strength. The transition occurs around $W = 0.16$.

and riddled with defects, indicating that the long-range stripe order is lost. The remaining short-range stripes become randomly orientated. In the relatively weak disorder region $0 < W < 0.1$, the whole structure of the density-density correlation function $S_0(\mathbf{q})$ is found to be similar to the clean system case, indicating the robustness of the CDW order. In Fig. 3(d), we plot the peak value $S_0(\mathbf{q}^*)$ as a function of W . The peak value $S_0(\mathbf{q}^*)$ remains nearly constant for relatively weak disorder $W < 0.1$. It starts to drop quickly around $W = 0.13$ and becomes comparable with the background value 0.5 at $W > 0.16$. Thus $W = 0.16$ is determined as the critical disorder strength, where the long-range CDW order becomes unstable.

The transport property of the above anisotropic CDW state is studied by calculating the Thouless energy $\Delta E_{\tau\tau}$ ($\tau = x$ or y), i.e., the ground-state energy difference due to a change of the boundary condition in the τ direction from periodic to antiperiodic, which is related to the longitudinal conductance in the x or y direction. We find that for a weak disorder, e.g., $W = 0.02$, ΔE_{yy} is about 50 times smaller than ΔE_{xx} , suggesting a large transport anisotropy associated with the quantum Hall stripe phase, which can be used to identify the stripe phase experimentally.

We further study the ground state at lower filling factors in the $N = 3$ LL. For $\nu = 1/3$ and $N_e = 8$, the low-energy states are found to become nearly degenerate in two different aspect ratio regions. The ground-state pair correlation functions corresponding to these two regions are plotted in Figs. 4(a) and 4(b), where the aspect ratio is taken to be $\text{asp} = 0.65$ and $\text{asp} = 0.86$, respectively. In the region

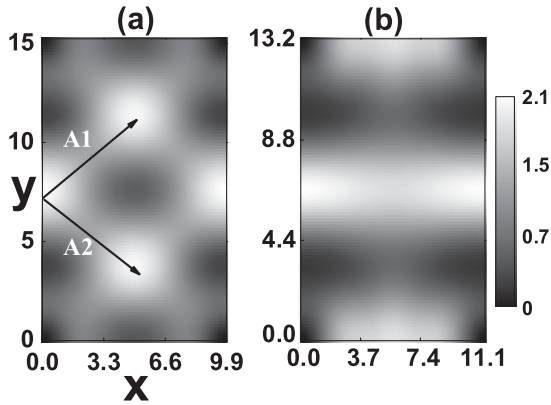


FIG. 4. Ground-state pair correlation functions for the $N = 3$ LL with $\nu = 1/3$ and $N_e = 8$ at two aspect ratios: (a) $\text{asp} = 0.65$ and (b) $\text{asp} = 0.86$.

around $\text{asp} = 0.65$, the ground state is a bubblelike CDW phase [19]. The bubbles distribute in a superlattice structure with the lattice vectors \mathbf{A}_1 and \mathbf{A}_2 . For $\text{asp} = 0.65$, we have $A_1 = A_2 = 6.24$, and the angle between the two lattice vectors is $\theta = 75^\circ$. Within the unit cell, there exist four bubbles and each bubble contains two electrons. In the region around $\text{asp} = 0.86$, the ground state is a stripe phase, and the stripe separation is about $D_s = 6.62$ for $\text{asp} = 0.86$. These results indicate that both the two-electron bubble phase and the stripe phase can be separately realized, depending on the geometry of the system. This is different from the case for nonrelativistic 2DES's, where usually only a single CDW phase exists at a given filling factor in a given LL [19]. More competing phases in the Dirac LL may be explained as a result of the special structure of the Dirac LL, which is essentially a combination of the $N = 2$ and $N = 3$ nonrelativistic LLs.

In summary, we have shown that various CDW phases can be realized in the partially filled $N = 3$ LL in graphene, the character of which can be explained from the mixture property of the electron wave functions of the Dirac LL. The CDW phases are robust against moderate disorder scattering. The unidirectional CDW stripe phase at half-filling shows large transport anisotropy, which can be measured experimentally.

This work is supported by the DOE Grant No. DE-FG02-06ER46305, the NSF Grants No. DMR-0605696 (D.N.S.) and No. DMR-0611562 (H.W., D.N.S.), the National Basic Research Program of China No. 2007CB925104 (L.S.), the NSF under MRSEC Grant No. DMR-0213706 at the Princeton Center for Complex Materials (FDMH), and the support from KITP (through NSF Grant No. PHY05-51464) and KITPC.

- [1] K. S. Novoselov *et al.*, *Science* **306**, 666 (2004); C. Berger *et al.*, *J. Phys. Chem. B* **108**, 19912 (2004).
- [2] Y. Zhang, J.P. Small, W.V. Pontius, and P. Kim, *Appl. Phys. Lett.* **86**, 073104 (2005); Y. Zhang, J.P. Small, M.E.S. Amori, and P. Kim, *Phys. Rev. Lett.* **94**, 176803 (2005).
- [3] K. S. Novoselov *et al.*, *Nature (London)* **438**, 197 (2005).
- [4] Y. Zhang, Y.-W. Tan, H.L. Stormer, and Philip Kim, *Nature (London)* **438**, 201 (2005).
- [5] V.P. Gusynin and S.G. Sharapov, *Phys. Rev. Lett.* **95**, 146801 (2005).
- [6] Y. Zhang *et al.*, *Phys. Rev. Lett.* **96**, 136806 (2006).
- [7] N.M.R. Peres, F. Guinea, and A.H. Castro Neto, *Phys. Rev. B* **73**, 125411 (2006).
- [8] E. McCann and V.I. Fal'ko, *Phys. Rev. Lett.* **96**, 086805 (2006).
- [9] Y. Zheng and T. Ando, *Phys. Rev. B* **65**, 245420 (2002).
- [10] F.D.M. Haldane, *Phys. Rev. Lett.* **61**, 2015 (1988).
- [11] D.N. Sheng, L. Sheng, and Z. Y. Weng, *Phys. Rev. B* **73**, 233406 (2006).
- [12] K. Nomura and A.H. MacDonald, *Phys. Rev. Lett.* **96**, 256602 (2006).
- [13] J. Alicea and M.P.A. Fisher, *Phys. Rev. B* **74**, 075422 (2006); K. Yang, S. Das Sarma, and A.H. MacDonald, *Phys. Rev. B* **74**, 075423 (2006); C. Toke and J.K. Jain, arXiv:cond-mat/0701026; M.O. Goerbig, R. Moessner, and B. Doucot, *Phys. Rev. B* **74**, 161407(R) (2006).
- [14] V.M. Apalkov and T. Chakraborty, *Phys. Rev. Lett.* **97**, 126801 (2006).
- [15] L. Sheng, D.N. Sheng, F.D.M. Haldane, and L. Balents, arXiv:cond-mat/07060371.
- [16] A.A. Koulakov, M.M. Fogler, and B.I. Shklovskii, *Phys. Rev. Lett.* **76**, 499 (1996); M.M. Fogler, A.A. Koulakov, and B.I. Shklovskii, *Phys. Rev. B* **54**, 1853 (1996); R. Moessner and J.T. Chalker, *ibid.* **54**, 5006 (1996).
- [17] H.A. Fertig, *Phys. Rev. Lett.* **82**, 3693 (1999); E. Fradkin and S.A. Kivelson, *Phys. Rev. B* **59**, 8065 (1999); A.H. MacDonald and M.P.A. Fisher, *Phys. Rev. B* **61**, 5724 (2000).
- [18] E.H. Rezayi, F.D.M. Haldane, and K. Yang, *Phys. Rev. Lett.* **83**, 1219 (1999); E.H. Rezayi and F.D.M. Haldane, *ibid.* **84**, 4685 (2000).
- [19] F.D.M. Haldane, E.H. Rezayi, and K. Yang, *Phys. Rev. Lett.* **85**, 5396 (2000).
- [20] M.P. Lilly *et al.*, *Phys. Rev. Lett.* **82**, 394 (1999); R.R. Du *et al.*, *Solid State Commun.* **109**, 389 (1999); J.P. Eisenstein, K.B. Cooper, L.N. Pfeiffer, and K.W. West, *Phys. Rev. Lett.* **88**, 076801 (2002).
- [21] C.-H. Zhang and Y.N. Joglekar, *Phys. Rev. B* **75**, 245414 (2007).
- [22] F.D.M. Haldane, *Phys. Rev. Lett.* **55**, 2095 (1985).
- [23] D.N. Sheng, Z. Wang, and B. Friedman, *Phys. Rev. B* **66**, 161103(R) (2002).
- [24] N. Shibata and D. Yoshioka, *Phys. Rev. Lett.* **86**, 5755 (2001).